NPHP4 Variants Are Associated With Pleiotropic Heart Malformations

Vanessa M. French,* Ingrid M.B.H. van de Laar,* Marja W. Wessels, Christan Rohe, Jolien W. Roos-Hesselink, Guangliang Wang, Ingrid M.E. Frohn-Mulder, Lies-Anne Severijnen, Bianca M. de Graaf, Rachel Schot, Guido Breedveld, Edwin Mientjes, Marianne van Tienhoven, Elodie Jadot, Zhengxin Jiang, Annemieke Verkerk, Sigrid Swagemakers, Hanka Venselaar, Zohreh Rahimi, Hossein Najmabadi, Hanne Meijers-Heijboer, Esther de Graaff, Wim A. Helbing, Rob Willemsen, Koen Devriendt, John W. Belmont, Ben A. Oostra, Jeffrey D. Amack,† Aida M. Bertoli-Avella†

Rationale: **Congenital heart malformations are a major cause of morbidity and mortality, especially in young children. Failure to establish normal left-right (L-R) asymmetry often results in cardiovascular malformations and other laterality defects of visceral organs.**

Objective: **To identify genetic mutations causing cardiac laterality defects.**

Methods and Results: **We performed a genome-wide linkage analysis in patients with cardiac laterality defects from a consanguineous family. The patients had combinations of defects that included dextrocardia, transposition of great arteries, double-outlet right ventricle, atrioventricular septal defects, and caval vein abnormalities. Sequencing of positional candidate genes identified mutations in *NPHP4*. We performed mutation analysis of *NPHP4* in 146 unrelated patients with similar cardiac laterality defects. Forty-one percent of these patients also had laterality defects of the abdominal organs. We identified 8 additional missense variants that were absent or very rare in control subjects. To study the role of *nphp4* in establishing L-R asymmetry, we used antisense morpholinos to knockdown *nphp4* expression in zebrafish. Depletion of *nphp4* disrupted L-R patterning as well as cardiac and gut laterality. Cardiac laterality defects were partially rescued by human *NPHP4* mRNA, whereas mutant *NPHP4* containing genetic variants found in patients failed to rescue. We show that *nphp4* is involved in the formation of motile cilia in Kupffer's vesicle, which generate asymmetrical fluid flow necessary for normal L-R asymmetry.**

Conclusions: ***NPHP4*** **mutations are associated with cardiac laterality defects and heterotaxy. In zebrafish, *nphp4* is essential for the development and function of Kupffer's vesicle cilia and is required for global L-R patterning. (*Circ Res*. 2012;110:1564-1574.)**

Key Words: congenital heart malformations ■ heterotaxy ■ *nphp4* ■ cilia ■ zebrafish

Laterality defects refer to a broad group of disorders caused by the disruption of normal left-right (L-R) asymmetry of the thoracic or abdominal visceral organs.[1] *Situs inversus totalis* is the mirror image reversal of all visceral organs, whereas heterotaxy is the abnormal orientation of one or more organs along the L-R axis.[2] In heterotaxy, congenital heart malformations result in major morbidity and mortality.[3] Although heterotaxy most often occurs as a

Original received March 22, 2012; revision received April 17, 2012; accepted April 23, 2012. In March 2012, the average time from submission to first decision for all original research papers submitted to *Circulation Research* was 13.2 days.

From the Department of Clinical Genetics, Erasmus Medical Center, Rotterdam, The Netherlands (V.M.F., I.M.B.H.v.d.L., M.W.W., C.R., L.-A.S., B.M.d.G., R.S., G.B., E.M., M.v.T., R.W., B.A.O., A.M.B.-A.); the Department of Cardiology, Erasmus Medical Center, Rotterdam, The Netherlands (J.W.R.-H.); State University of New York, Upstate Medical University, Department of Cell and Developmental Biology, Syracuse, NY (G.W., J.D.A.); the Department of Pediatric Cardiology, Erasmus Medical Center-Sophia, Rotterdam, The Netherlands (I.M.E.F.-M., W.A.H.); Lille University of Sciences and Technologies, Lille, France (E.J.); the Department of Molecular and Human Genetics, Baylor College of Medicine, Houston, TX (Z.J., J.W.B.); the Department of Bioinformatics, Erasmus Medical Center, Rotterdam, The Netherlands (A.V., S.S.); the Department of Genetics, Erasmus Medical Center, Rotterdam, The Netherlands (S.S.); Center for Molecular and Biomolecular Informatics (CMBI) and Nijmegen Center for Molecular Life Sciences (NCMLS), Radboud University Nijmegen Medical Center, The Netherlands (H.V.); Medical Biology Research Center and Biochemistry Department, Medical School, Kermanshah University of Medical Sciences, Kermanshah, Iran (Z.R.).; Genetics Research Center, University of Social Welfare and Rehabilitation Sciences, Tehran, Iran (H.N.); the Department of Clinical Genetics, VU Medical Center, Amsterdam, The Netherlands (H.M.-H.); the Department of Cell Biology, Faculty of Science, Utrecht University, Utrecht, The Netherlands (E.d.G.); and the Department of Clinical Genetics, University Hospital Leuven, Leuven, Belgium (K.D.).

*These authors contributed equally. †These authors share senior authorship.

The online-only Data Supplement is available with this article at http://circres.ahajournals.org/lookup/suppl/doi:10.1161/CIRCRESAHA.112.269795/-/DC1.

Correspondence to A.M. Bertoli-Avella, MD, Department of Clinical Genetics, Erasmus MC Rotterdam, PO Box 2040, 3000 CA, Rotterdam, The Netherlands. E-mail a.bertoliavella@erasmusmc.nl

sporadic condition, familial clustering has been documented with pedigrees suggesting autosomal recessive, autosomal dominant and X-linked inheritance.[4–7]

L-R patterning of vertebrate embryos occurs before organ formation and is conducted by a conserved signaling cascade that includes asymmetrical expression of the *NODAL*, *LEFTY,* and *PITX2* genes in left lateral plate mesoderm (LPM).[8] Motile cilia are involved in establishing this L-R asymmetrical signaling. Laterality defects have been linked to ciliary motility by the observation that 48% of individuals with primary cilia dyskinesia also had *situs inversus totalis* and 6% had heterotaxy.[9]

Animal models have assisted our understanding of L-R patterning and the role of cilia. The *inversus viscerum* (*iv*) mouse has a mutation in the ciliary *left-right dynein* (*lrd*) gene and often develops laterality defects.[10] *Lrd* was found to be required for normal motility of monocilia on an embryonic structure called the node. These node cilia generate a leftward fluid flow that is necessary for normal asymmetrical Nodal-Lefty-Pitx2 signaling.[11] In zebrafish, Kupffer's vesicle (KV) is a ciliated organ analogous to the mouse node that is essential for normal L-R patterning.[12] Asymmetrical fluid flow generated by the monocilia may move signaling factors[11,13] and/or bend mechanosensory cilia[14] to initiate asymmetrical signaling.

Dysfunction of ciliary proteins gives rise to a wide range of human disorders known as ciliopathies. They can lead to a variety of defects including craniofacial, skeletal, respiratory, reproductive, renal, visual, olfactory, and auditory abnormalities.[15–17] The nephronophthisis (NPHP) and associated ciliopathies—Senior-Loken syndrome (SLSN), Joubert syndrome, and Meckel-Gruber syndrome—are characterized by cilia-related defects, including cystic kidney disease, retinal degeneration, liver fibrosis, and brain malformations.[18,19] Mutations in 18 genes are known to cause nephronophthisis and associated ciliopathies.[20,21] Interestingly, mutations in *NPHP2/INVS* and *NPHP3* can also lead to heterotaxy, *situs inversus,* and isolated congenital heart malformations.[22–24]

Protein network analysis has shown that several of these proteins form an interaction network organized in at least 3 connected modules: NPHP1–4 to 8, NPHP5–6, and MKS.[25] Ciliary localization analysis of eight nephrocystins (NPHP1–6, 9, and 10) indicates that they are present in the primary cilia, the basal body and/or the centrioles and suggest that they participate in ciliary assembly and trafficking.[25–28]

In this study, a genome-wide linkage analysis identified *nephronophthisis-4* (*NPHP4*) variants in patients with cardiac laterality defects. Functional studies indicated that loss of zebrafish *nphp4* resulted in cardiac laterality defects. In addition, *nphp4* depletion disrupted asymmetrical nodal expression in the LPM, indicating *nphp4* is required for global L-R patterning of the embryo. Analysis of cilia in KV revealed that loss of *nphp4* reduced cilia length and disrupted asymmetrical fluid flow. Our results establish the importance of *nphp4* in cilia development and function. Furthermore, our findings suggest that malfunction of *NPHP4* contributes to a wide range of congenital heart malformations and more complex defects within the heterotaxy spectrum.

Non-standard Abbreviations and Acronyms

AS	aortic stenosis
ASD	atrial septal defect
AVSD	atrioventricular septal defect
CoA	coarctation of the aorta
KV	Kupffer's vesicle
LOD scores	logarithm of the odds
LPM	lateral plate mesoderm
L-R	left-right
MO	morpholino oligonucleotides
NPHP	nephronophthisis
PDA	persistent ductus arteriosus
PS	pulmonary valve stenosis
SB-MO	splicing blocking MO
SLSN	Senior-Loken syndrome
TB-MO	translation blocking MO
TGA	transposition of great arteries (dextro or levo)
VSD	ventricular septal defect
wt	wild-type

Methods

Patients

We studied a large consanguineous family of Iranian origin (Figure 1A) with complex consanguinity loops. This family was followed by us during many years. The healthy parents of branch 1 and 2 are double first-degree cousins; the mothers of these parents are sisters and the fathers are brothers. The healthy parents of branch 3 are first-degree cousins (their mothers are sisters) and related to the other 2 branches via the mothers (all mothers are sisters). In this family, 5 patients were born with congenital cardiac defects, of which 3 had cardiac laterality defects (IV-1, IV-8, IV-12).

A total of 146 DNA samples from patient cohorts with heart (and other organs) laterality defects were collected. Patient samples were collected at the Erasmus Medical Center, Rotterdam, The Netherlands (15 samples), the Department of Clinical Genetics, University Hospital Leuven, Belgium (36 samples), and from the Baylor College of Medicine, Houston, TX (95 samples).

An expanded Methods section describing all procedures is available in the Online Data Supplement.

Results

Clinical Studies

We identified a consanguineous family including 5 patients with congenital heart malformations. Three patients (IV-1, IV-8, and IV-12; Figure 1A) were born with similar cardiac laterality defects (Table). Patient IV-1 had dextrocardia, atrial situs solitus, complete atrioventricular septal defect, and discordant ventriculoarterial connection with dextro-transposition of the great arteries (d-TGA). In addition, he had an interrupted inferior caval vein and a severe pulmonary valve stenosis (PS). He had no surgical correction and died suddenly at the age of 22 years. No autopsy was performed. Patient IV-8 had dextrocardia, dextrorotation, and atrial situs solitus. She had an azygos continuation of the right infrahepatic part of the inferior caval vein draining into the right superior caval vein and the suprahepatic part of the inferior caval vein draining into the right atrium. She had a cor

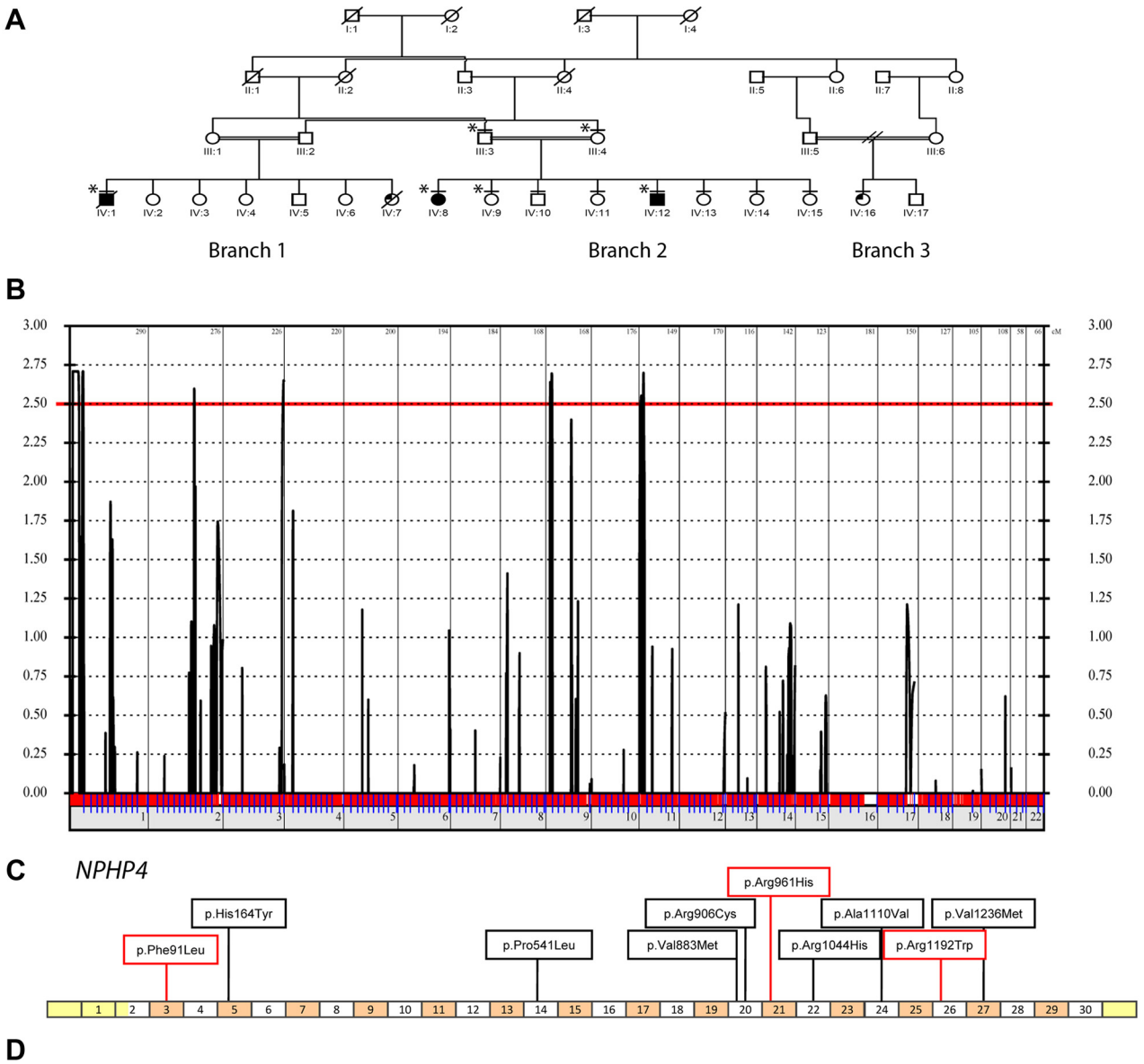

	p.Phe91Leu	p.His164Tyr	p.Pro541Leu	p.Val883Met	p.Arg906Cys	p.Arg961His	p.Arg1044His	p.Ala1110Val	p.Arg1192Trp	p.Val1236Met
Homo sapiens	RIV**F**NEP	ALL**H**PLL	QEF**P**LEA	LAD**V**DSE	DVS**R**ESD	YRE**R**TKA	FHL**R**G-S	LFR**A**SGG	GEP**R**DIF	LQR**V**DVS
Mus musculus	RIT**F**NEP	ALL**H**PLL	AESVLES	LAD**V**DSE	AAGQEAD	YRE**R**TKA	FHL**R**G-S	LFRVETG	GEP**R**DVF	LQR**V**DVS
Equus caballus	RIV**F**NEP	ALL**H**PRL	QEL**P**LQG	LAD**V**DSE	GAG**R**EGD	YRE**R**TKA	FHLQG-G	LFR**A**SGG	GEP**R**DVF	LQR**V**DVS
Bos taurus	RIV**F**NEP	ALL**H**PLL	-EF**P**LEG	LAD**V**DSE	GINQEGD	YRE**R**TKA	FHL**R**G-S	LFR**A**GSG	GEP**R**DVF	LQR**V**DVS
Canis familiaris	RII**F**DEP	ALL**H**PLL	-EP**P**SEG	LAD**V**DRE	GAC**R**EGD	YRE**R**TKA	FHL**R**G-S	LFRGSGG	REP**R**DVF	LQR**V**DVS
Rattus norvegicus	RIL**F**NEP	ALL**H**PLL	AGSVLES	LAD**V**DSE	AVGQEAD	YRE**R**TKA	FHL**R**G-S	LFRVETG	GEP**R**DVF	LQR**V**DVS
Danio rerio	RVL**F**NEV	ALL**H**PTL	VER**P**VVG	LPEINSE	--GAEEK	YRE**R**CKT	FHLKEKT	LFRGEDR	GEPQDVY	LQRMDLS

Figure 1. Genome-wide Linkage Analysis (GWLA) and *NPHP4* variants identification. A, Simplified genealogical tree of the index family. A horizontal line above the symbol indicates medical examination. **Open symbols** indicate normal individuals, **solid black symbols** indicate patients with cardiac laterality defects, and **quarter-filled symbols** indicate presence of other congenital heart malformations. The double line between individuals indicates consanguinity and the diagonal line through a symbol is a deceased family member. Individuals labeled with an **asterisk** were included in the GWLA. For the genetic analysis, all individuals in whom medical examination was not possible were considered as "phenotype unknown." **B**, Multipoint LOD scores: *X*-axis represents all human autosomes and *Y*-axis corresponds to the LOD scores. Chromosomal regions with LOD scores above 2.5 (red horizontal line) were further investigated. **C**, Summary of the *NPHP4* variations identified in patients of the index family, the Dutch and the American cohorts. White and peach-colored boxes represent exons; yellow boxes represent untranslated regions. Red-boxed variants were previously described in SLSN4 or NPHP4 patients. **D**, Alignment of NPHP4 protein with several species. The illustrated protein segments were derived from Ensembl reference sequences. Red letters indicate amino acid residues identical to those of human.

Table. *NPHP4* Variants Found in Patients With Cardiovascular Malformations With or Without Laterality Defects of Other Thoracic or Abdominal Organs

Patient Details				Clinical Features			*NPHP4* Genotypes				Frequency in Control Subjects†
Family	Origin	Patient	Sex	Cardiovascular Abnormalities	Other Organs Asymmetry	Other Features	Coding Variant	Protein Effect	Doses	Prediction*	
1	Iranian	IV-1	M	Dextrocardia, D-TGA, ASD, VSD, AVSD, PS, interrupted ICV	. . .	. . .	c.3131G>A	p.Arg1044His	Hom‖¶	Pathogenic	0.2% (2/1232) 0.01% (1/6887)
							c.3706G>A	p.Val1236Met	Hom‖¶	Neutral	0.1% (1/1232) 0%
1	Iranian	IV-8	F	Dextrocardia, ASD, VSD, interrupted ICV with azygous continuation, persistent left SCV and ICV, cor triatriatum	Left lung isomerism	. . .	c.3131G>A	p.Arg1044His	Hom‖¶	Pathogenic	0.2% (2/1232) 0.01% (1/6887)
							c.3706G>A	p.Val1236Met	Hom‖¶	Neutral	0.1% (1/1232) 0%
1	Iranian	IV-12	M	D-TGA, DORV, VSD, PDA	. . .	. . .	c.3131G>A	p.Arg1044His	Hom‖¶	Pathogenic	0.2% (2/1232) 0.01% (1/6887)
							c.3706G>A	p.Val1236Met	Hom‖¶	Neutral	0.1% (1/1232) 0%
1	Iranian	IV-16	F	VSD, PS, PDA	. . .	. . .	c.3131G>A	p.Arg1044His	Het	Pathogenic	0.2% (2/1232) 0.01% (1/6887)
							c.3706G>A	p.Val1236Met	Het	Neutral	0.1% (1/1232) 0%
2	Dutch, Chinese	02D3049	F	VSD, PA	Right lung isomerism, abdominal situs inversus	Large splenic cyst	c.3329C>T	p.Ala1110Val	Het	Neutral	0.6% (2/318) 0.8% (56/6872) rs139767853
3	Dutch, Cape Verde	07D2466	F	Dextrocardia, AVSD, PS, L-TGA, DORV	Right lung isomerism, midline liver, asplenia	. . .	c.1622C>T	p.Pro541Leu	Het	Pathogenic	0% (0/182) 0.3% (30/9810)** rs145255635
4	Caucasian	LAT0025	M	Mesocardia	Abdominal situs inversus; midline liver and intestinal malrotation	Cholelithiasis, omphalocele, small spleen	c.271T>C	p.Phe91Leu‡	Het	Pathogenic	0% (0/180) 0.1% (10/6766)
5	Caucasian	LAT0033	F	Mesocardia, atrial inversion, VSD, ASD, PA, D-TGA, DORV, severe aortic root dilation	Abdominal situs inversus; midline liver	. . .	c.490C>T	p.His164Tyr	Het‖	Pathogenic	0% (0/180) 0%
6	Caucasian	LAT1268	M	HLHS, VSD, ASD, MV hypoplasia, BAV, CoA, PDA, interrupted ICV with azygous continuation	Polysplenia, transverse liver, midline gall bladder and portal vein, intestinal malrotation	Right hydronephrosis	c.2647G>A	p.Val883Met	Het¶	Neutral	0% (0/122) 0.01% (1/6897)
7	Caucasian	LAT0079	M	Common atrium, right atrial isomerism, single ventricle, AVSD, PA, azygous continuation to right SCV	Abdominal situs inversus	. . .	c.2716 C>T	p.Arg906Cys	Het	Pathogenic	0% (0/122) 0%
8	Caucasian	LAT1168	M	Right atrial isomerism, single ventricle, ASD, MV atresia, PS, DORV, VSD, infra-diaphragmatic TAPVR, absent ICV with azygous continuation to ipsilateral SCV, persistent left SCV to coronary sinus, right aortic arch with a common brachiocephalic trunk, abnormal branching pattern of the abdominal vessels from the aorta	Abdominal situs inversus, asplenia and intestinal malrotation	. . .	c.2882G>A	p.Arg961His§	Het‖	Pathogenic	0.5% (1/182) 0.4% (30/6952)
9	Hispanic	LAT0145	M	HLHS, AVSD, D-TGA, DORV, bicuspid PV, PS, supracardiac TAPVR	Midline liver, asplenia and intestinal malrotation	Mild hepatomegaly with calcifications, cholelithiasis; hypothyroidism	c.3574C>T	p.Arg1192Trp§	Het¶	Pathogenic	0% (0/182) 0.3% (21/6625) rs139022622
10	Caucasian	LAT1034	M	Single ventricle, MV atresia, VSD, ASD, subvalvular AS, PS, L-TGA, DORV, PDA	. . .	. . .	c.3329C>T	p.Ala1110Val	Het	Neutral	0.6% (2/318) 0.8% (56/6872) rs139767853

ASD indicates atrial septal defect; VSD, ventricular septal defect; AVSD, atrioventricular septal defect; MV, mitral valve; TGA, transposition of great arteries (dextro or levo); DORV, double-outlet right ventricle; PDA, persistent ductus arteriosus; BAV, bicuspid aortic valve; AS, aortic stenosis; PA, pulmonary atresia; PV, pulmonary valve; PS, pulmonary valve stenosis; HLHS, hypoplastic left heart syndrome; CoA, coarctation of the aorta; TAPVR, total anomalous pulmonary venous return; ICV, inferior caval vein; SCV, superior caval vein; Het, heterozygous; and Hom, homozygous.

All variants are absent or rare (<1%) in control populations.

*Prediction of the genetic variant effect on protein level (Pmut, SNPs3D, SIFT, PolyPhen, HOPE).

†Based on ethnically matched (in house) control chromosomes and the frequencies reported by the NHLBI Exome Sequencing Project.

‡Reported in patients with *SLSN4*.

§Reported in patients with *NPHP4*.

‖Inherited from father.

¶Inherited from mother.

**Total allele counts include European and African American population.

triatriatum with the right pulmonary veins draining into the right part of the left atrium and the left pulmonary veins into the left part of the left atrium. A persistent left inferior and superior caval vein also drained into the left part of the left atrium. She had a secundum atrial septal defect (ASD) and perimembranous ventricular septal defect (VSD). She had also left bronchial isomerism. Patient IV-12 had atrial situs solitus, atrioventricular concordance, and ventriculoarterial discordance namely, double-outlet right ventricle and d-TGA. He also had a subpulmonary VSD, patent foramen ovale, and patent ductus arteriosus (PDA).

In addition, patient IV-7 died shortly after birth due to an unspecified congenital heart malformation (Figure 1A). The fifth patient (IV-16) had mild congenital heart malformations consisting of a small VSD, PS, and PDA, which was ligated at 1 year of age (Table).

Physical examination revealed no dysmorphisms and all patients had normal psychomotor development. CT/MRI or ultrasound of the abdomen revealed no kidney cysts and all individuals have reached adulthood at the time of their last evaluations. No abdominal laterality defects such as asplenia or polysplenia, malrotation of the gut, or midline liver were detected in any of these cases. None of the patients had signs of abnormal mucociliary clearance. No visual problems or night blindness were reported.

Genome-Wide Linkage Analysis

The genome-wide linkage analysis was performed using Affymetrix SNP arrays. Two unaffected parents, 3 patients and 1 healthy sibling (Figure 1A) were included in the analysis. Multipoint linkage analysis revealed 5 regions on chromosomes 1, 2, 3, 9, and 11 with logarithm of the odds (LOD) scores above 2.5 (Figure 1B). The maxLOD scores (2.7) were located on chromosome 1p36 and 11p15. Subsequently, microsatellite markers mapping to all candidate regions were tested. The loci on chromosomes 2, 3, and 9 were excluded, based on heterozygosity observed in the patients (data not shown).

On the chromosome 1p36 locus, all three patients with cardiac laterality defects (IV-1, IV-8, and IV-12) shared a homozygous region covered by 59 SNPs from rs4845835 to rs1203695. Haplotype analysis showed recombinations that delimited the borders of the region from rs2722782 (5.26 Mb) to rs1203696 (14.21 Mb) (Online Figure I, A). Thus, the candidate region spanned 9 Mb and contained 152 genes (NCBI build 37.1). These patients also showed homozygous genotypes for 49 consecutive SNPs on chromosome 11, from rs16905816 to rs10500752. Further fine mapping in the 11p area delineated the borders of the linkage region between markers D11S4188 (telomeric) and rs2896598 (centromeric) (Online Figure I, B). The chromosome 11 locus extended only 3 Mb (9.1–12.1 Mb), containing 34 genes (NCBI build 37.1).

Haplotypes from both loci were examined in all available family members. A normal person (IV-14, with normal MRI of the thorax/abdomen) had homozygous haplotypes on the chromosome 1 locus (Online Figure I, A). In addition, individuals IV-3 and IV-4 were homozygotes for the chromosome 11 locus (Online Figure I, B); both persons were reported as unaffected, but medical examinations could not be performed. Patient IV-16, exhibiting a mild cardiac phenotype and no laterality defects, carried heterozygous haplotypes at both loci (data not shown). Only the 3 patients with laterality heart defects had homozygous haplotypes on both loci. Since these were the only genomic regions where the 3 patients showed extended homozygosity, we further investigated these loci.

Sequence Analysis

A total of 109 genes on the chromosome 1p36 locus had a known reference sequence (NCBI build 37.1). Selection of genes for sequence analysis was based on available expression and/or functional information. The data were analyzed through the use of Ingenuity pathway analysis (Ingenuity Systems). Thirty-six candidate genes were selected from the chromosome 1 locus. Direct sequencing of their coding regions identified 2 homozygous missense variants in the *NPHP4* gene present in three patients from the index family: c.3131G>A (p.Arg1044His) and c.3706G>A (p.Val1236Met) (Online Table I). These nonsynonymous variants are extremely rare in the Iranian (Kurdish) population (allele frequency of 0.2% and 0.1% in 1232 control chromosomes). Moreover, the variants were absent in 270 Caucasian/Dutch and 178 Hispanic control chromosomes.

From the 34 genes mapping to the chromosome 11 locus, 19 genes had a well annotated reference sequence. Sequence analysis of their coding regions and exon-intron boundaries revealed only 1 novel DNA missense variant (Online Table I). In the *AMPD3* gene (*adenosine monophosphate deaminase 3*), the homozygous c.2240 G>A (p.Arg747Gln) variant was found. This variant was not present in 626 control chromosomes. Mutations in the *AMPD3* gene lead to (asymptomatic) deficiency of erythrocyte AMP deaminase[29] (OMIM 612874).

NPHP4 Variants in Patients With Laterality Defects (Heterotaxy)

We sequenced all 30 exons of *NPHP4* in 3 cohorts of patients with cardiac laterality defects—with or without other situs abnormalities. Patient samples were collected at the Erasmus Medical Center, Rotterdam, the Department of Clinical Genetics, Leuven, and from Baylor College of Medicine, Houston, TX. All 146 patients had a variety of cardiac laterality defects. Transposition of the great arteries was the most frequently found (49% of the patients). In addition, complete atrioventricular septal defect, double-outlet right ventricle, and abnormal pulmonary venous return were often reported. Dextrocardia was present in 33% of patients. Moreover, 41% had documented laterality defects of the abdominal organs, including abdominal situs inversus, asplenia or polysplenia, midline liver, and intestinal malrotation.

Nine missense variants were found in 10 patients (Figure 1C and 1D and Table). The population frequency of each allele was tested by sequencing ethnically matched control subjects. A variant was considered as likely nonpathogenic if the allele frequency in healthy individuals was higher than 1%. Thus, p.Pro1160Leu with a frequency of 2.1% in control chromosomes was excluded from further analysis. In addition, we investigated the frequency of these variants in available databases (dbSNP135, 1000Genomes, NHLBI ex-

ome project). All variants were very rare or absent in control subjects (allele frequency ≤0.8%; Table).

These rare *NPHP4* variants were significantly more frequent in heterotaxy cases (6%, 9 of 146 cases) than in control subjects (1.2%, 3 of 250, Fisher exact test $P=0.006$). In silico evaluation was performed using five prediction computer programs. This assessment predicted the impact of amino acid substitutions on the structure and function of human proteins. The variants were classified as probably pathogenic if at least 3 programs considered them as damaging (Table). Seven variants satisfied this criterion. Interestingly, p.Phe91Leu, p.Arg961His, and p.Arg1192Trp have been reported in patients with SLSN type 4 or nephronophthisis type 4.[30]

Identification of Zebrafish *nphp4* and Characterization of Its Expression During Embryogenesis

A zebrafish *nphp4* ortholog was taken from the Ensembl database (Online Figure II). To determine the pattern of *nphp4* expression during embryogenesis, we performed reverse transcription PCR (RT-PCR) and RNA in situ hybridization experiments at several developmental stages. Consistent with a recent report[31] we found *nphp4* expression was maternally supplied and ubiquitously expressed during the first 24 hours of zebrafish development (Online Figure III, B through G). RT-PCR detected *nphp4* expression at all stages tested between 4-cell stage and 100 hours postfertilization (hpf) (Online Figure III, A). This early and ubiquitous expression pattern suggested a role for *nphp4* during early development.

nphp4 Is Required for Normal Cardiac Laterality in Zebrafish

To assess the function of *nphp4* during embryonic development, we used antisense morpholino oligonucleotides (MO) to knockdown expression of zebrafish Nphp4 protein. Embryos injected with a MO designed to block *nphp4* mRNA translation (*nphp4* TB-MO) developed dose-dependent morphological abnormalities reminiscent of embryos with cilia defects,[32–34] including a curved body axis (Online Figure IV, D) and otolith formation defects at 2 days postfertilization (dpf) (Online Figure V, A and B).

In addition, RNA in situ hybridization staining of the heart-specific marker *cmlc2* revealed heart laterality defects. Uninjected controls and embryos injected with a standard control MO showed normal rightward looping of the heart at 2 dpf (Figure 2A and 2B). However, heart looping in *nphp4* TB-MO injected embryos was significantly altered, as the heart often looped in the reverse orientation or failed to loop (Figure 2A and 2B).

To test whether heart laterality phenotypes were specific to knockdown of *nphp4*, we designed 2 additional MOs to interfere with *nphp4* mRNA splicing at exon 4 (*nphp4* SB-MO1) or exon 9 (*nphp4* SB-MO2) (Online Figure IV, A and B). Quantitative RT-PCR analysis indicated *nphp4* SB-MO1 reduced *nphp4* mRNA levels by 90% (Online Figure IV, C) and caused heart laterality defects without inducing body axis defects (Figure 2A and 2B and Online Figure IV, D). This indicates heart L-R phenotypes are separable from axial defects. *nphp4* SB-MO2 reduced the amount of normally spliced *nphp4* mRNA by 50% (Online Figure IV, C) and resulted in curved body axis and heart looping defects (Online Figure IV, D, and Figure 2A and 2B, respectively), similar to *nphp4* TB-MO injected embryos. Injecting a lower dose of *nphp4* SB-MO2 (0.4 ng) also altered heart looping, but with reduced penetrance (Figure 2B), suggesting partial loss of *nphp4* can cause cardiac laterality defects.

Other abnormalities such as hydrocephalus or gross eye defects were not observed. At 5 dpf, pronephric cysts were observed with a low penetrance in embryos injected with TB-MO (11%) or SB-MO2 (8%) (Online Figure V, C and D). No pronephric cysts were observed in SB-MO1–injected embryos. Our results using 3 independent MOs suggested a role for *nphp4* that is required for normal heart laterality in zebrafish.

To further confirm that defects observed in zebrafish embryos were specifically due to *nphp4* depletion, we conducted rescue experiments using human wild-type (wt) *NPHP4* mRNA. Coinjecting *nphp4* TB-MO with wt *NPHP4* mRNA resulted in a partial, but significant, rescue of heart looping defects (percentage of normal embryos improved from 43% to 60%, $P=0.03$; Figure 2C). Next, we coinjected *nphp4* TB-MO with human *NPHP4* mRNA containing either the c.3131G>A (p.Arg1044His) or c.3706G>A (p.Val1236Met) missense variant identified in the index family. In contrast to wt *NPHP4*, these *NPHP4* variants failed to rescue heart looping defects (Figure 2C). These results suggest that these variants are pathogenic and are involved in human laterality defects.

nphp4 Controls Global L-R Patterning of the Zebrafish Embryo

To determine whether *nphp4* plays a role in heart laterality specifically or is involved in establishing global L-R patterning of the embryo, we analyzed additional markers of L-R asymmetry. RNA in situ hybridization, using *foxa3* probes to label the embryonic gut, showed that *nphp4* knockdown significantly altered laterality of the liver and pancreas in *nphp4* MO injected embryos (Figure 3A and 3B). We next analyzed expression of the Nodal-related gene *southpaw* (*spaw*), the earliest asymmetrically expressed gene in LPM in zebrafish.[35] Control embryos exhibited normal left-sided *spaw* expression (Figure 3C and 3D). In contrast, *nphp4* MO injected embryos showed a significant disruption of *spaw* expression, which was often reversed, bilateral, or absent (Figure 3C and 3D). Altered asymmetrical gene expression can result from defects in the embryonic midline.[36] However, analysis of the midline markers *no tail* and *sonic hedgehog* revealed that midline structures were intact in *nphp4* MO–injected embryos (Online Figure VI). These results indicate *nphp4* functions independent of midline development to control *spaw* expression and global L-R patterning of the embryo.

nphp4 Is Required for Normal Cilia Length and Directional Fluid Flow in KV

In zebrafish, KV is a transient organ that generates cilia-driven asymmetrical fluid flow necessary to bias *spaw* expression to the left LPM. Examination of live embryos at the

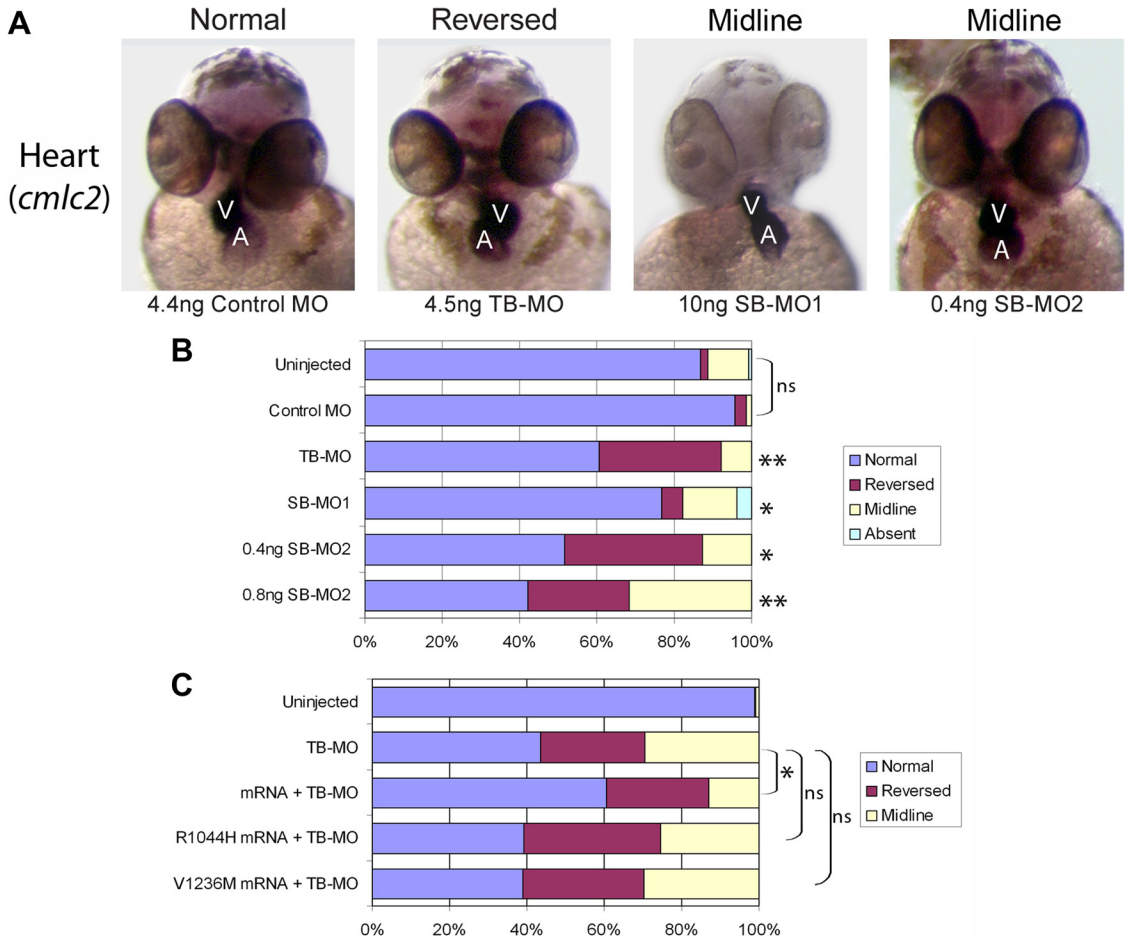

Figure 2. *nphp4* knockdown alters zebrafish heart laterality. A, In situ hybridizations using a heart-specific probe (*cmlc2*) showed that embryos injected with a control MO had predominantly normal cardiac looping. In contrast, heart laterality was often reversed or remained along the midline in *nphp4* MO injected embryos. V indicates ventricle; A, atrium. **B**, The distributions of heart orientation observed in uninjected embryos (n=242), Control MO (n=71), *nphp4* TB-MO (n=89), *nphp4* SB-MO1 (n=106), and *nphp4* SB-MO2 (0.8 ng, n=76; 0.4 ng, n=95) embryos. **C**, Wild-type but not mutant human *NPHP4* mRNA partially rescued zebrafish heart laterality defects; the graph shows the distribution of normal and abnormal heart looping in uninjected embryos (n=239), embryos injected with 4.5 ng TB-MO (n=154), and injected with both 100 pg human wt *NPHP4* mRNA and 4.5 ng TB-MO (n=249). In contrast, mutant *NPHP4* containing either the p.Arg1044His (n=189) or p.Val1236Met (n=188) missense variants failed to rescue the phenotype (4.5 ng TB-MO and 100 pg mutant *NPHP4* mRNA). *$P \leq 0.038$, **$P \leq 2.6 \times 10^{-4}$; ns indicates not significant.

8 somite stage showed that the KV organ appeared normal in control MO (Figure 4A) and *nphp4* MO–injected embryos (Figure 4B and 4C). However, analysis of cilia in KV by fluorescent immunostaining with acetylated Tubulin antibodies revealed that the cilia were significantly shorter in *nphp4* MO–injected embryos (Figure 4E through 4G) as compared with controls (Figure 4D and 4G). We did not observe a significant difference of KV cilia number between control and *nphp4* MO–injected embryos (Figure 4H). To analyze KV cilia function, we injected fluorescent beads into KV of live embryos and used video microscopy to record fluid flow.[12] Most control embryos showed strong counterclockwise asymmetrical fluid flow (Figure 4I and Online Movie I). In contrast, flow was often absent (Figure 4J and 4L and Online Movie II) or reduced (Figure 4K and 4L and Online Movie III) in *nphp4* MO–injected embryos. Consistent with dose-dependent effects of *nphp4* SB-MO2 on heart looping (Figure 2B), we observed more severe flow defects in embryos injected with a higher *nphp4* SB-MO2 dose (Figure 4L). Together, these results show that *nphp4* knockdown results in short KV cilia and compromises asymmetrical fluid flow that is necessary for normal L-R patterning.

Discussion

We found homozygous missense *NPHP4* variants in a consanguineous family containing 3 patients with cardiac laterality defects, bronchial isomerism, and normal abdominal situs. Interestingly, though *NPHP4* is a cilia related gene that is mutated in patients with autosomal recessive juvenile nephronophthisis (NPHP type 4, OMIM 606966)[37] and SLSN (SLSN4, OMIM 606996),[38] our patients did not show signs of nephronophthisis or retinitis pigmentosa, which are distinctive features of these diseases.

Because of the known interaction between NPHP1, NPHP2/INVS, NPHP3, and NPHP4 proteins,[23–24,37] it is obvious that mutations in one or more of these genes disrupt the same pathway(s) and can lead to similar phenotypes (ie, nephronophthisis). Conversely, mutations within the same gene can lead to various phenotypic outcomes in different

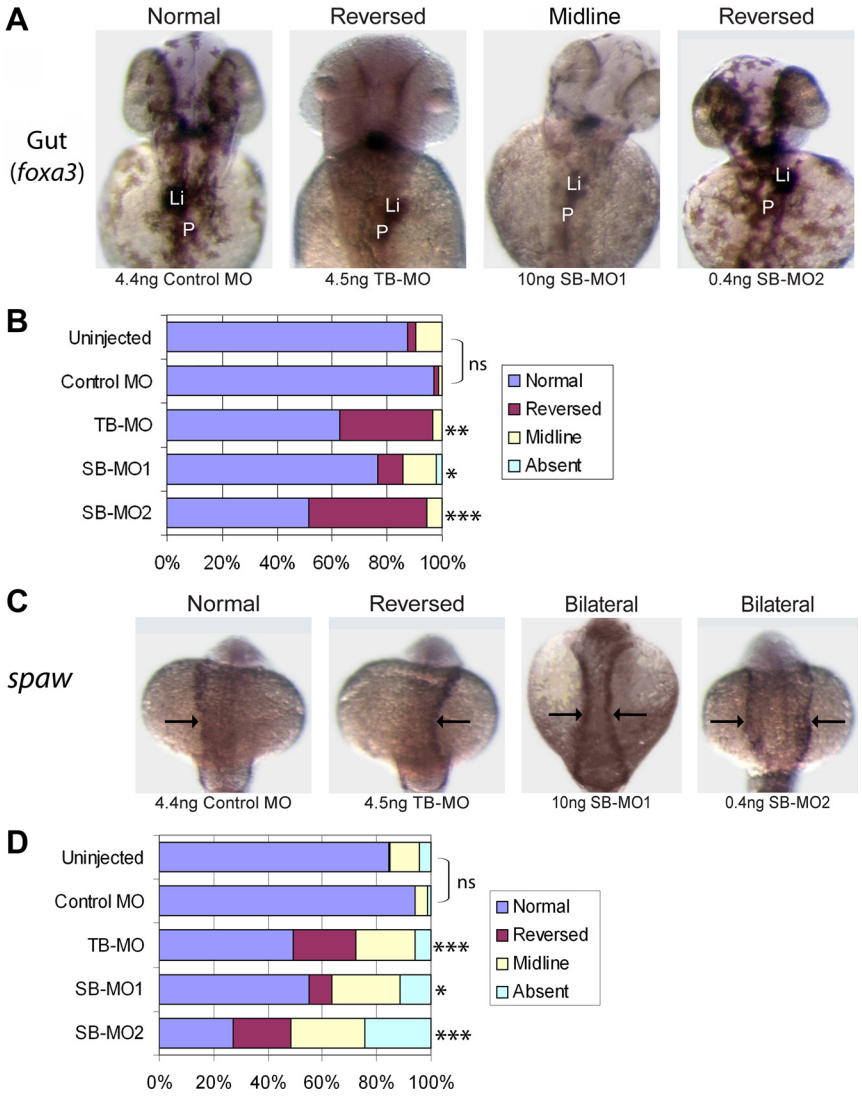

Figure 3. *nphp4* knockdown alters zebrafish gut laterality and disrupts global asymmetrical gene expression. **A**, In situ hybridizations using a gut-specific probe (*foxa3*) showed that embryos injected with a control MO had predominantly normal liver and pancreas orientation. In contrast, gut laterality was often reversed or remained along the midline in *nphp4* MO injected embryos. Li indicates liver; P, pancreas. **B**, Distributions of gut orientation observed in uninjected embryos (n=242), control MO (n=71), *nphp4* TB-MO (n=89), *nphp4* SB-MO1 (n=106), and *nphp4* SB-MO2 (n=76) injected embryos. **C**, In situ hybridization staining of *southpaw* (*spaw*) expression (**arrows**) in lateral plate mesoderm at 16 to 18 SS. *spaw* expression, which is normally left-sided in controls was often reversed, bilateral, or absent in *nphp4* MO–injected embryos. **D**, Distributions of *spaw* expression patterns in uninjected embryos (n=217), control MO (n=88), *nphp4* TB-MO (n=134), *nphp4* SB-MO1 (n=116), and *nphp4* SB-MO2 (n=70) embryos. $^{*}P \leq 0.028$, $^{**}P \leq 0.0012$, and $^{***}P \leq 5.9 \times 10^{-4}$; ns indicates not significant.

patients. Mutations in *NPHP2* result in nephronophthisis with or without situs inversus and mild cardiac defects,[23] whereas *NPHP3* mutations lead to isolated nephronophthisis or retinal degeneration.[39] Alternately, *NPHP3* mutations can cause a broad clinical spectrum of early embryonic patterning defects comprising situs inversus, congenital heart defects, central nervous system malformations, and renal-hepatic-pancreatic dysplasia.[24] The *NPHP6* gene (*CEP290*) is another good example. The phenotypic spectrum of the mutations ranges from isolated blindness, SLSN, nephronophthisis, Joubert syndrome, Bardet-Biedl syndrome, to the lethal Meckel-Grüber syndrome.[40]

We investigated the presence of *NPHP4* variants in 146 sporadic patients having cardiac laterality defects, with or without involvement of other thoracic or abdominal organs. In 6% of the patients, we identified heterozygous missense variants compared with 1.2% of the ethnically matched control subjects, indicating mutation excess in the patients ($P<0.006$). No compound heterozygous or homozygous variants were detected in these sporadic cases. Similarly, single heterozygous *NPHP4* variants were found in the majority of patients with autosomal recessive nephronophthisis type 4.[30] A second mutation might be located in an area not covered by exon sequencing or in another (cilia-related) gene. The latest, a complex genetic model with combined effects of multiple genes, seems to be the most plausible explanation. In fact, di- or oligogenic inheritance have been demonstrated in several ciliopathies, including the nephronophthisis,[21,41] Joubert syndrome,[42] and Bardet-Biedl syndrome.[43–44]

The findings in our study are entirely consistent with a complex, oligogenic disease model. The rare heterozygous variants identified in the sporadic cases have probably an epistatic effect with additional genetic modifiers. Even in the index consanguineous family, we cannot exclude the existence of other genetic variants that explain the complex cardiovascular malformations and heterotaxy and the lack of renal/visual disease.

In congenital heart malformations and heterotaxy, the NODAL signaling pathway is a paradigm for oligogenic inheritance. Some patients with heterotaxy and/or conotruncal defects such as double-outlet right ventricle and TGA, show several mutations in genes belonging to the NODAL signaling pathway.[45,46] As functional significance of mutations in these genes were demonstrated, the cumulative

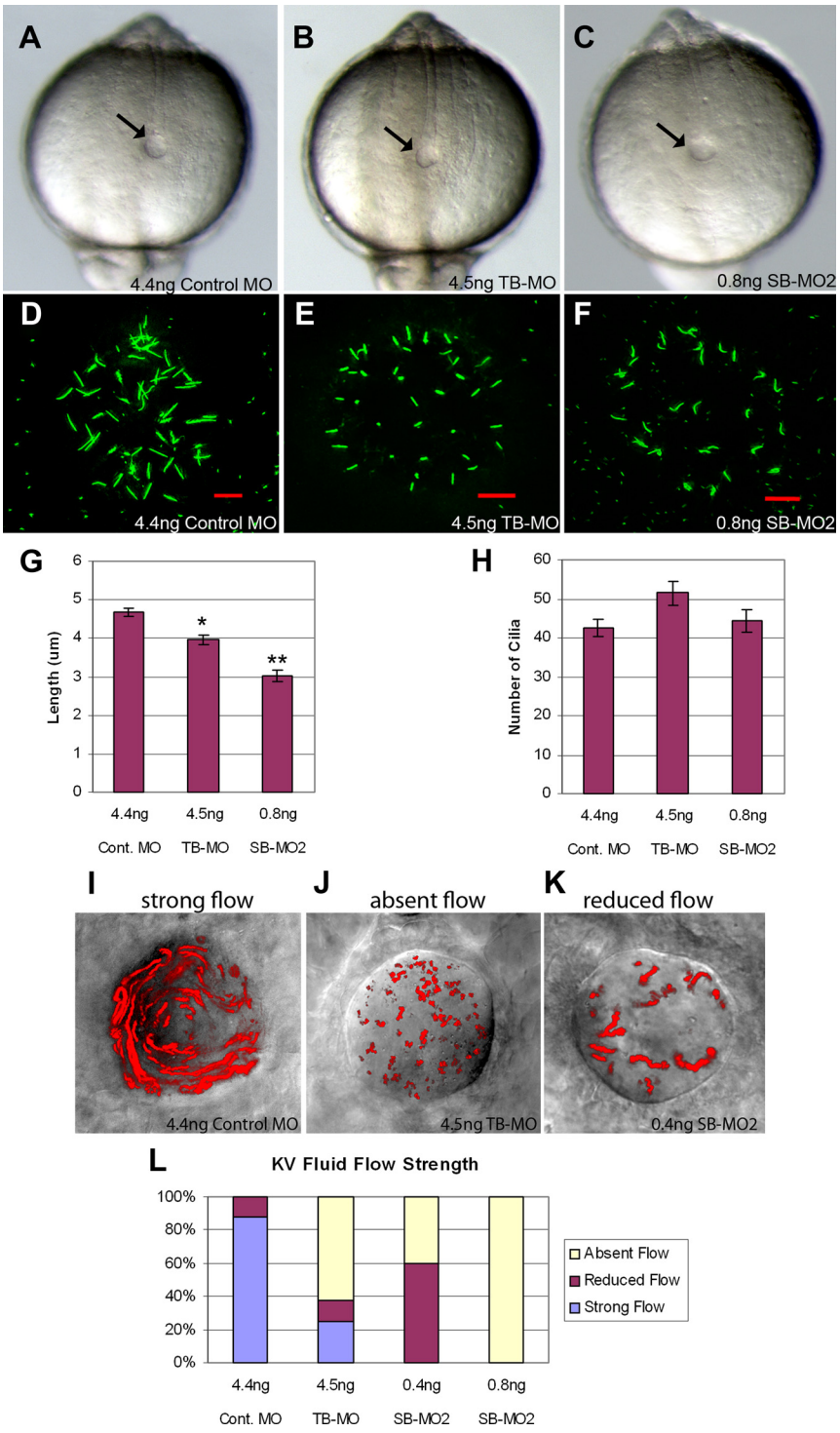

Figure 4. *nphp4* knockdown shortens cilia and disrupts fluid flow in Kupffer's vesicle (KV). A through **C**, KV (**arrow**) appeared similar in live control MO (**A**), *nphp4* TB-MO (**B**), and *nphp4* SB-MO2 (**C**) embryos at 8 SS. **D** through **F**, Visualization of KV cilia using antiacetylated tubulin antibodies at 8 SS revealed shorter cilia in *nphp4* MO embryos (**E** and **F**), relative to controls (**D**). Red scale bar represents 10 microns. **G** and **H**, Graphs show the average KV cilia length (**G**) and number (**H**) in control MO (n=38), *nphp4* TB-MO (n=21), and *nphp4* SB-MO2 (n=25) embryos at 8 SS. Error bars represent standard error of the mean. $^{*}P<0.0001$ and $^{**}P<3\times10^{-12}$ when compared with control MO embryos (Student *t* test). **I** through **K**, Fluorescent bead paths (red) superimposed on images of KV of representative embryos at 8 to 10 SS. Strong directional flow (**I**) was observed in most control MO injected embryos (**I**), whereas flow was often absent (**J**) or reduced (**K**) in *nphp4* TB-MO and *nphp4* SB-MO2 embryos. **L**, The percentage of embryos classified with a strong, reduced, or absent fluid flow. Embryos were injected with control MO (n=17), *nphp4* TB-MO (n=8), 0.4 ng (lower dose) *nphp4* SB-MO2 (n=5), or 0.8 ng *nphp4* SB-MO2 (n=4).

effects of multiple mutations may lead to reduced NODAL signaling eventually resulting in congenital heart malformations. In addition independent combinatorial roles of the NODAL signaling pathway and *ZIC3* gene have been demonstrated in familial TGA patients.[47] These studies support the notion that genetic variants or susceptibility alleles within 1 or more developmental pathways may dysregulate signaling in a synergistic fashion and cause congenital heart malformations or heterotaxy.

Studies in humans, zebrafish, and mice indicate that *NPHP2* and *NPHP3* play a role in L-R axis determination.[22–24,39] To investigate the role of *NPHP4* in establishing L-R asymmetry, we used antisense MOs to knockdown expression of zebrafish *nphp4*. Depletion of *nphp4* in zebrafish resulted in abnormal heart and gut orientation, closely resembling the (cardiac) laterality defects observed in the patients. Coinjection of *nphp4* TB-MO and human wt *NPHP4* mRNA significantly ameliorated the phenotypic spectrum due to *nphp4*

depletion. In contrast, coinjection of *nphp4* TB-MO and human *NPHP4* mRNA containing genetic variants found in patients failed to rescue the laterality defects suggesting that these variants are pathogenic. Furthermore, analysis of asymmetrical gene expression revealed that *nphp4* knockdown alters asymmetrical Nodal expression in the LPM without affecting expression of midline markers.

Our analyses in zebrafish have confirmed that knockdown of *nphp4* results in shortened motile cilia.[48] For first time, we show that *nphp4* depletion leads to disruption of cilia-driven fluid flow within KV, which probably causes laterality defects. Similarly, *nphp3* knockdown in zebrafish leads to *situs inversus* and heterotaxy due to defective (fewer and shorter) KV cilia.[49]

In conclusion, we identified *NPHP4* mutations in patients with cardiac laterality defects and other malformations within the heterotaxy spectrum. In zebrafish, our results demonstrate that *nphp4* is required for global L-R patterning of the embryo via regulation of Nodal signaling and plays a role that is essential for the development and function of KV cilia.

The linking of *NPHP4* to L-R axis determination and laterality defects will help dissect the complex genetic composition of heterotaxy and related cardiovascular malformations.

Acknowledgments

We are grateful to the family and patients and who participated in the study. We thank Fiona Foley, Chunlei Gao, and Herma van der Linde for excellent technical assistance and Tom de Vries Lentsch for the artwork. We acknowledge Prof Peter van der Spek for the use of Ingenuity Systems.

Sources of Funding

This work was partially funded by the Dutch Heart Foundation, The Netherlands (2006T006), to I.M.B.H.v.d.L., an Erasmus MC grant, and an Erasmus Fellowship (Erasmus Medical Center, The Netherlands) to A.M.B.-A., a grant from the Center for Biomedical Genetics (CBG), The Netherlands to B.A.O., and a grant from the National Heart, Lung, and Blood Institute (R01HL095690) to J.D.A.

Disclosures

None.

References

1. Bisgrove BW, Morelli SH, Yost HJ. Genetics of human laterality disorders: insights from vertebrate model systems. *Annu Rev Genomics Hum Genet*. 2003;4:1–32.
2. Jacobs JP, Anderson RH, Weinberg PM, et al. The nomenclature, definition and classification of cardiac structures in the setting of heterotaxy. *Cardiol Young*. 2007;17(Suppl 2):1–28.
3. Sutherland MJ, Ware SM. Disorders of left-right asymmetry: heterotaxy and situs inversus. *Am J Med Genet C Semin Med Genet*. 2009;151C: 307–317.
4. Belmont JW, Mohapatra B, Towbin JA, Ware SM. Molecular genetics of heterotaxy syndromes. *Curr Opin Cardiol*. 2004;19:216–220.
5. Gebbia M, Ferrero GB, Pilia G, Bassi MT, Aylsworth A, Penman-Splitt M, Bird LM, Bamforth JS, Burn J, Schlessinger D, Nelson DL, Casey B. X-linked situs abnormalities result from mutations in zic3. *Nat Genet*. 1997;17:305–308.
6. Vitale E, Brancolini V, De Rienzo A, Bird L, Allada V, Sklansky M, Chae CU, Ferrero GB, Weber J, Devoto M, Casey B. Suggestive linkage of situs inversus and other left-right axis anomalies to chromosome 6p. *J Med Genet*. 2001;38:182–185.
7. Wessels MW, De Graaf BM, Cohen-Overbeek TE, et al. A new syndrome with noncompaction cardiomyopathy, bradycardia, pulmonary stenosis, atrial septal defect and heterotaxy with suggestive linkage to chromosome 6p. *Hum Genet*. 2008;122:595–603.
8. Zhu L, Belmont JW, Ware SM. Genetics of human heterotaxias. *Eur J Hum Genet*. 2006;14:17–25.
9. Kennedy MP, Omran H, Leigh MW, et al. Congenital heart disease and other heterotaxic defects in a large cohort of patients with primary ciliary dyskinesia. *Circulation*. 2007;115:2814–2821.
10. Supp DM, Witte DP, Potter SS, Brueckner M. Mutation of an axonemal dynein affects left-right asymmetry in inversus viscerum mice. *Nature*. 1997;389:963–966.
11. Nonaka S, Tanaka Y, Okada Y, Takeda S, Harada A, Kanai Y, Kido M, Hirokawa N. Randomization of left-right asymmetry due to loss of nodal cilia generating leftward flow of extraembryonic fluid in mice lacking kif3b motor protein. *Cell*. 1998;95:829–837.
12. Essner JJ, Amack JD, Nyholm MK, Harris EB, Yost HJ. Kupffer's vesicle is a ciliated organ of asymmetry in the zebrafish embryo that initiates left-right development of the brain, heart and gut. *Development*. 2005; 132:1247–1260.
13. Tanaka Y, Okada Y, Hirokawa N. FGF-induced vesicular release of sonic hedgehog and retinoic acid in leftward nodal flow is critical for left-right determination. *Nature*. 2005;435:172–177.
14. McGrath J, Somlo S, Makova S, Tian X, Brueckner M. Two populations of node monocilia initiate left-right asymmetry in the mouse. *Cell*. 2003; 114:61–73.
15. Baker K, Beales PL. Making sense of cilia in disease: the human ciliopathies. *Am J Med Genet C Semin Med Genet*. 2009;151C:281–295.
16. Bisgrove BW, Yost HJ. The roles of cilia in developmental disorders and disease. *Development*. 2006;133:4131–4143.
17. Fliegauf M, Benzing T, Omran H. When cilia go bad: cilia defects and ciliopathies. *Nat Rev Mol Cell Biol*. 2007;8:880–893.
18. Hildebrandt F, Attanasio M, Otto E. Nephronophthisis: disease mechanisms of a ciliopathy. *J Am Soc Nephrol*. 2009;20:23–35.
19. Hildebrandt F, Zhou W. Nephronophthisis-associated ciliopathies. *J Am Soc Nephrol*. 2007;18:1855–1871.
20. Hurd TW, Hildebrandt F. Mechanisms of nephronophthisis and related ciliopathies. *Nephron Exp Nephrol*. 2011;118:e9–e14.
21. Otto EA, Ramaswami G, Janssen S, et al. Mutation analysis of 18 nephronophthisis associated ciliopathy disease genes using a DNA pooling and next generation sequencing strategy. *J Med Genet*. 2010; 10:10.
22. Chaki M, Hoefele J, Allen SJ, Ramaswami G, Janssen S, Bergmann C, Heckenlively JR, Otto EA, Hildebrandt F. Genotype-phenotype correlation in 440 patients with nphp-related ciliopathies. *Kidney Int.* 2011; 80:1239–1245.
23. Otto EA, Schermer B, Obara T, et al. Mutations in invs encoding inversin cause nephronophthisis type 2, linking renal cystic disease to the function of primary cilia and left-right axis determination. *Nat Genet*. 2003;34: 413–420.
24. Bergmann C, Fliegauf M, Bruchle NO, et al. Loss of nephrocystin-3 function can cause embryonic lethality, Meckel-Gruber-like syndrome, situs inversus, and renal-hepatic-pancreatic dysplasia. *Am J Hum Genet*. 2008;82:959–970.
25. Sang L, Miller JJ, Corbit KC, et al. Mapping the nphp-jbts-mks protein network reveals ciliopathy disease genes and pathways. *Cell*. 2011;145: 513–528.
26. Shiba D, Manning DK, Koga H, Beier DR, Yokoyama T. Inv acts as a molecular anchor for nphp3 and nek8 in the proximal segment of primary cilia. *Cytoskeleton*. 2010;67:112–119.
27. Shiba D, Yokoyama T. The ciliary transitional zone and nephrocystins. *Differentiation*. 2011;12:12.
28. Shiba D, Yamaoka Y, Hagiwara H, Takamatsu T, Hamada H, Yokoyama T. Localization of inv in a distinctive intraciliary compartment requires the c-terminal ninein-homolog-containing region. *J Cell Sci*. 2009;122: 44–54.
29. Yamada Y, Goto H, Ogasawara N. A point mutation responsible for human erythrocyte amp deaminase deficiency. *Hum Mol Genet*. 1994;3: 331–334.
30. Hoefele J, Sudbrak R, Reinhardt R, Lehrack S, Hennig S, Imm A, Muerb U, Utsch B, Attanasio M, O'Toole JF, Otto E, Hildebrandt F. Mutational analysis of the nphp4 gene in 250 patients with nephronophthisis. *Hum Mutat*. 2005;25:411.
31. Slanchev K, Putz M, Schmitt A, Kramer-Zucker A, Walz G. Nephrocystin-4 is required for pronephric duct-dependent cloaca formation in zebrafish. *Hum Mol Genet*. 2011;20:3119–3128.
32. Kramer-Zucker AG, Olale F, Haycraft CJ, Yoder BK, Schier AF, Drummond IA. Cilia-driven fluid flow in the zebrafish pronephros, brain

and Kupffer's vesicle is required for normal organogenesis. *Development*. 2005;132:1907–1921.
33. Colantonio JR, Vermot J, Wu D, Langenbacher AD, Fraser S, Chen JN, Hill KL. The dynein regulatory complex is required for ciliary motility and otolith biogenesis in the inner ear. *Nature*. 2009;457:205–209.
34. Gao C, Wang G, Amack JD, Mitchell DR. Oda16/wdr69 is essential for axonemal dynein assembly and ciliary motility during zebrafish embryogenesis. *Dev Dyn*. 2010;239:2190–2197.
35. Long S, Ahmad N, Rebagliati M. The zebrafish nodal-related gene southpaw is required for visceral and diencephalic left-right asymmetry. *Development*. 2003;130:2303–2316.
36. Tabin CJ. The key to left-right asymmetry. *Cell*. 2006;127:27–32.
37. Mollet G, Salomon R, Gribouval O, Silbermann F, Bacq D, Landthaler G, Milford D, Nayir A, Rizzoni G, Antignac C, Saunier S. The gene mutated in juvenile nephronophthisis type 4 encodes a novel protein that interacts with nephrocystin. *Nat Genet*. 2002;32:300–305.
38. Otto E, Hoefele J, Ruf R, Mueller AM, Hiller KS, Wolf MT, Schuermann MJ, Becker A, Birkenhager R, Sudbrak R, Hennies HC, Nurnberg P, Hildebrandt F. A gene mutated in nephronophthisis and retinitis pigmentosa encodes a novel protein, nephroretinin, conserved in evolution. *Am J Hum Genet*. 2002;71:1161–1167.
39. Olbrich H, Fliegauf M, Hoefele J, Kispert A, Otto E, Volz A, Wolf MT, Sasmaz G, Trauer U, Reinhardt R, Sudbrak R, Antignac C, Gretz N, Walz G, Schermer B, Benzing T, Hildebrandt F, Omran H. Mutations in a novel gene, nphp3, cause adolescent nephronophthisis, tapeto-retinal degeneration and hepatic fibrosis. *Nat Genet*. 2003;34:455–459.
40. Coppieters F, Lefever S, Leroy BP, De Baere E. Cep290, a gene with many faces: mutation overview and presentation of cep290base. *Hum Mutat*. 2010;31:1097–1108.
41. Hoefele J, Wolf MT, O'Toole JF, Otto EA, Schultheiss U, Deschenes G, Attanasio M, Utsch B, Antignac C, Hildebrandt F. Evidence of oligogenic inheritance in nephronophthisis. *J Am Soc Nephrol*. 2007;18:2789–2795.
42. Tory K, Lacoste T, Burglen L, Moriniere V, Boddaert N, Macher MA, Llanas B, Nivet H, Bensman A, Niaudet P, Antignac C, Salomon R, Saunier S. High nphp1 and nphp6 mutation rate in patients with Joubert syndrome and nephronophthisis: potential epistatic effect of nphp6 and ahi1 mutations in patients with nphp1 mutations. *J Am Soc Nephrol*. 2007;18:1566–1575.
43. Katsanis N, Ansley SJ, Badano JL, Eichers ER, Lewis RA, Hoskins BE, Scambler PJ, Davidson WS, Beales PL, Lupski JR. Triallelic inheritance in Bardet-Biedl syndrome, a mendelian recessive disorder. *Science*. 2001; 293:2256–2259.
44. Katsanis N, Eichers ER, Ansley SJ, Lewis RA, Kayserili H, Hoskins BE, Scambler PJ, Beales PL, Lupski JR. Bbs4 is a minor contributor to Bardet-Biedl syndrome and may also participate in triallelic inheritance. *Am J Hum Genet*. 2002;71:22–29.
45. Roessler E, Ouspenskaia MV, Karkera JD, Velez JI, Kantipong A, Lacbawan F, Bowers P, Belmont JW, Towbin JA, Goldmuntz E, Feldman B, Muenke M. Reduced nodal signaling strength via mutation of several pathway members including foxh1 is linked to human heart defects and holoprosencephaly. *Am J Hum Genet*. 2008;83:18–29.
46. Mohapatra B, Casey B, Li H, Ho-Dawson T, Smith L, Fernbach SD, Molinari L, Niesh SR, Jefferies JL, Craigen WJ, Towbin JA, Belmont JW, Ware SM. Identification and functional characterization of nodal rare variants in heterotaxy and isolated cardiovascular malformations. *Hum Mol Genet*. 2009;18:861–871.
47. De Luca A, Sarkozy A, Consoli F, Ferese R, Guida V, Dentici ML, Mingarelli R, Bellacchio E, Tuo G, Limongelli G, Digilio MC, Marino B, Dallapiccola B. Familial transposition of the great arteries caused by multiple mutations in laterality genes. *Heart*. 2010;96:673–677.
48. Burckle C, Gaude HM, Vesque C, Silbermann F, Salomon R, Jeanpierre C, Antignac C, Saunier S, Schneider-Maunoury S. Control of the wnt pathways by nephrocystin-4 is required for morphogenesis of the zebrafish pronephros. *Hum Mol Genet*. 2011;20:2611–2627.
49. Zhou W, Dai J, Attanasio M, Hildebrandt F. Nephrocystin-3 is required for ciliary function in zebrafish embryos. *Am J Physiol Renal Physiol*. 2010;299:F55–F62.

Novelty and Significance

What Is Known?

- Failure to establish normal left-right (L-R) organ orientation during embryonic development results in congenital heart defects and other malformations of thoracic and abdominal organs (laterality defects).
- Congenital heart malformations are genetically heterogeneous and complex disorders.
- The zebrafish provides a useful animal model to investigate genes and mechanisms involved in establishing L-R asymmetry.

What New Information Does This Article Contribute?

- *NPHP4* genetic variants were identified for first time in patients with cardiac malformations with or without laterality defects of other visceral organs.
- In zebrafish embryos, depletion of *nphp4* expression leads to abnormal L-R organ patterning with abnormal heart looping and gut orientation.
- *Nphp4* is involved in the formation of motile cilia in Kupffer's vesicle, which generate directional fluid flow necessary for normal L-R axis determination.

This study describes the identification of *NPHP4* variants in patients with congenital heart malformations using a genome wide linkage analysis and gene sequencing in a consanguineous family. Subsequent *NPHP4* screening of sporadic cases with similar cardiac defects with or without malformations of other organs identified novel or rare variants in 6% of these patients. Depletion of *nphp4* expression in zebrafish embryos leads to abnormal heart and gut orientation resembling the phenotype observed in the patients. For the first time, we show that *nphp4* depletion leads to disruption of cilia-driven fluid flow, which probably causes laterality defects in zebrafish. Integration of the human genetics data and the functional work on zebrafish indicates that *NPHP4* malfunction contributes to a wide range of laterality defects, including complex heart malformations.